ASTRID reactor pin design

December 2, 2024

1 Initial Remarks

The project summed up in the following work has been done using Python (3.11.7) in IPython notebooks edited on Google Colab, Jupiter and VS Code. On a conceptual level, the analysis of the fuel pin was performed spatially from the outside inwards (radially) and the different phenomena taken into account are investigated, as much as possible, in the order in which it was expected that they would arise, from the beginning of the assembly in the core to its extraction. It is important to remark that this work follow the perspective of the single-channel analysis and we focused solely on the hottest pin of the hottest channel in order to have a conservative approach.

2 Cold Geometry

The first thing that was done at the beginning of the project was to perform an interpolation of the provided axial peak factor. The reasons to do so were two: having an axial power profile to integrate to obtain the axial temperature profile of the coolant and later on being able to decide in how many points we would want to investigate the temperature of the pin.
To do so, the axial peak factors were divided in five groups of contiguous values: values 1 to 4 are fitted with a constant (average value), 5 to 11 are fitted with a sin function plus a constant, 12 to 13 are fitted with a straight line, 14 to 19 are fitted with an other constant, the remaining ones are fitted with a parable.

Since methods like the minimization of the squared difference would often result in functions arguably non-employable for this analysis due to, for example, non-negligible overestimation of the maximum peak factor, the parameters of this curves were found by trial and error.
The result is displayed in the figure 3b. After calculating the coolant temperature, we decided to only perform the thermal analysis in proximity of the the thirty axial peak factors in order to have acceptable computation times.

After assuming single phase coolant and independent channels, the first step in the thermal analysis of the fuel pin is to consider the initial geometry of the pin unaffected by any phenomena. The mass flow rate "seen" by a pin is the total mass flow rate of the assembly divided by the number of pins (multiplied by two due to the hexagonal lattice of the pins). Since the the temperature of the coolant at the inlet is given and the correlation for the heat capacity was provided, the latter was implemented as a python function which was called in a python function returning $\frac{dT}{dz}|_{coolant}$, which was then integrated using *scipy.integrate.solve_ivp* with the inlet temperature as a boundary condition.

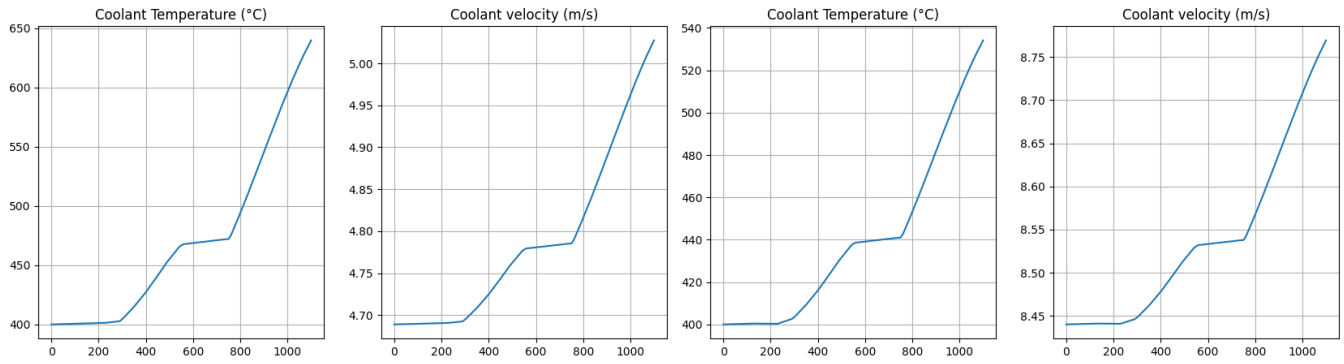

(a) With no throttling (b) With throttling

Figure 1: Temperature and velocity of the coolant vs pin active length (mm)

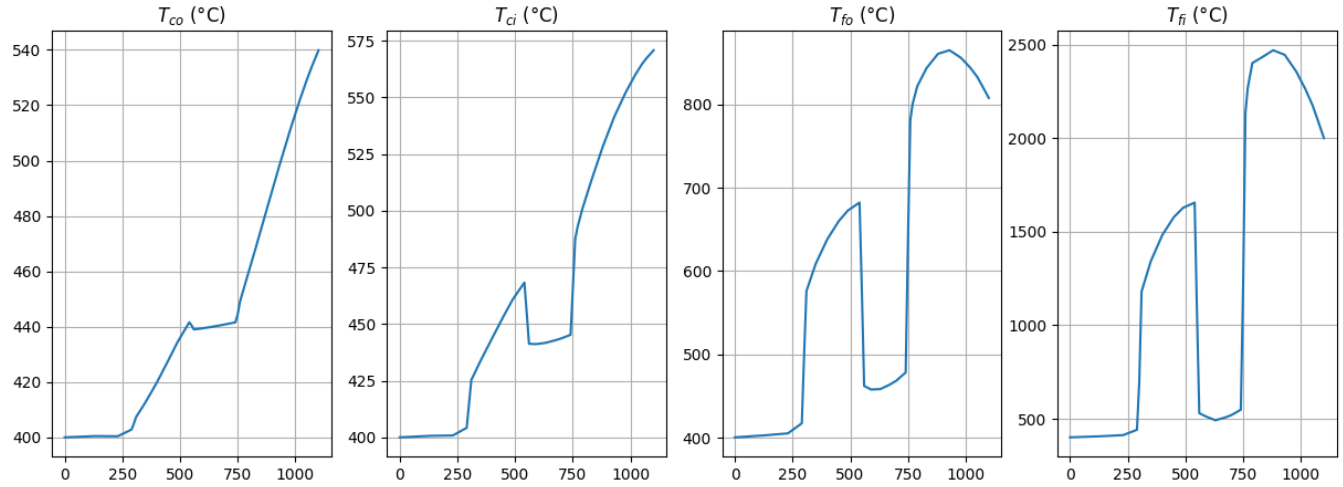

Figure 2: Cladding and fuel temperature vs active length (mm) in cold geometry

As displayed in figure 1a the temperature already exceeded the limitations for the cladding temperature, that would clearly be even higher. In order to tackle this issue, the use of the throttling was implemented simply as a constant (1.8) multiplying the mass flow rate. In figure 1b the temperature is shown to be way lower and the coolant velocity was still reasonable (less than 10 m/s).

Except for the coolant, an other important assumption has been made: no axial thermal conductivity.
After calculating the outer cladding temperature, a couple of issues arises. The temperature can be calculated as

$$T_{co} = T_{coolant} + \frac{q'}{2\pi R_{co} h} \tag{1}$$

$q'(z)$ is represented by an array of 30 values calculated as the product of the Axial peak factors and the maximum linear power provided. h is calculated as the ratio between the Nusselt number and the characteristic length of the pin, multiplied by the heat conductivity of the coolant. The correlation for the Nusselt number as a function of the Peclet number was provided, which is in turn a function of velocity, viscosity, density of the coolant and geometry of the problem:

$$Pe = \frac{\rho \mu L < v >}{k} \tag{2}$$

The cladding thickness was chosen by trial and error in compliance with the temperature design limits for both cladding and fuel. Greater thickness means better thermal dissipation but also higher probability to have mechanical issues because of the fuel-cladding contact due to the expansion of the material. We found out that the lower limit was given by the inner fuel temperature: with a thickness of 0.53 mm after the hot geometry (before restructuring) we obtained a temperature of 2397°C.
In order to have a safety margin, we chose a value of $0.55mm$.
Calculating the inner temperature, while not requiring the more complex correlations of the previous point, was trickier due to the the fact that the heat conductivity is a function of temperature, which is the unknown under investigation. The option were the integration of thirty ODEs that would portray precisely the temperature radial profile of the cladding at the thirty different values of z, or approximating the T of the cladding as the average of the inner and outer temperature. Since the first option required long computation time, the prospect of having to do so every time a similar problem would have arose was deemed unbearable and discarded.
The calculations for finding the outer fuel temperature are not very different from the latter, since while evaluating the heat exchange across the gap it was taken into account only the conduction term, thus making the gap resemble an other cylindrical shell. This could be done since the aim is verifying that the temperature of the fuel is below a given threshold because the approximation presented leads to an overestimation of the fuel temperature and is hence conservative. Moreover, the contact and radiative terms are often way smaller than the conduction. The heat conductivity of the filling gas (He) is a function of its temperature that is once again approximated as an average between the inner cladding temperature and outer fuel temperature.
Once the outer fuel temperature profile has been developed, the same can be done for the inner fuel temperature with some complications. First, some pellets are MOX pellets with a central hole ($0 - 300mm$ and $600 - 800mm$) and the others are made of natural uranium. Different materials have different heat conductivity, and these are a function of porosity (which in the beginning is 5% since the density of the material is 95%TD) and burnup, that in the beginning is null.

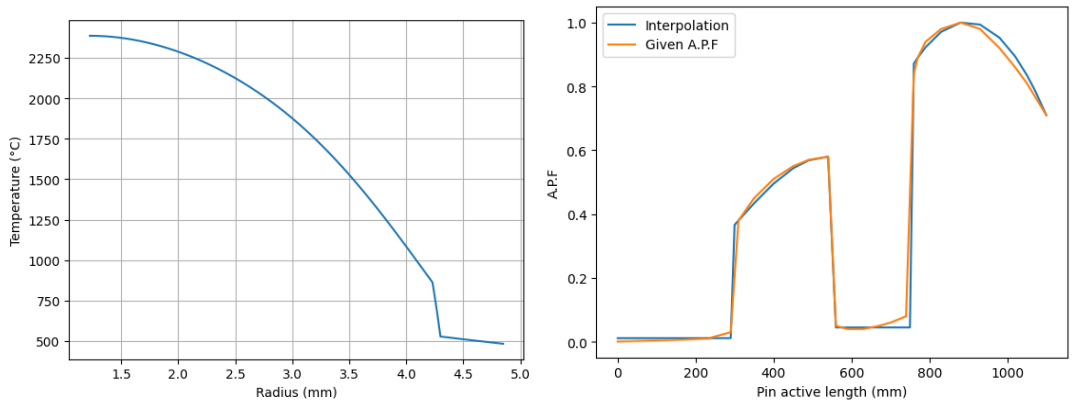

(a) Cold geometry radial profile

(b) A.P.F. fitting curve

Figure 3

In figure 2 the results of the cladding and fuel calculations are reported. It needs to be underlined that the maximum temperature of the fuel is way higher than the design limit, but, as shown in hot geometry later on, so high temperatures are never reached thanks to the thermal expansion of the materials.

3 Hot Geometry

The aim of the hot geometry is to estimate the change in geometry and subsequently in temperature due to the thermal expansion. The approximation that has been done was to deem constant the outer cladding temperature and calculating the expansions as functions once again of the average temperature of the inner and outer temperature of each "shell". Based on the temperatures of the cold geometry the expansions were estimated at each and everyone of the thirty points and the temperatures calculated again. This process was iterated with a while cycle that ended once the difference between the maximum temperatures of the fuel were minor than 1°C. The choice of the condition is dictated by the need to ensure that the design limits are respected in the most critical points, hence ensuring that the same limits are respected everywhere.

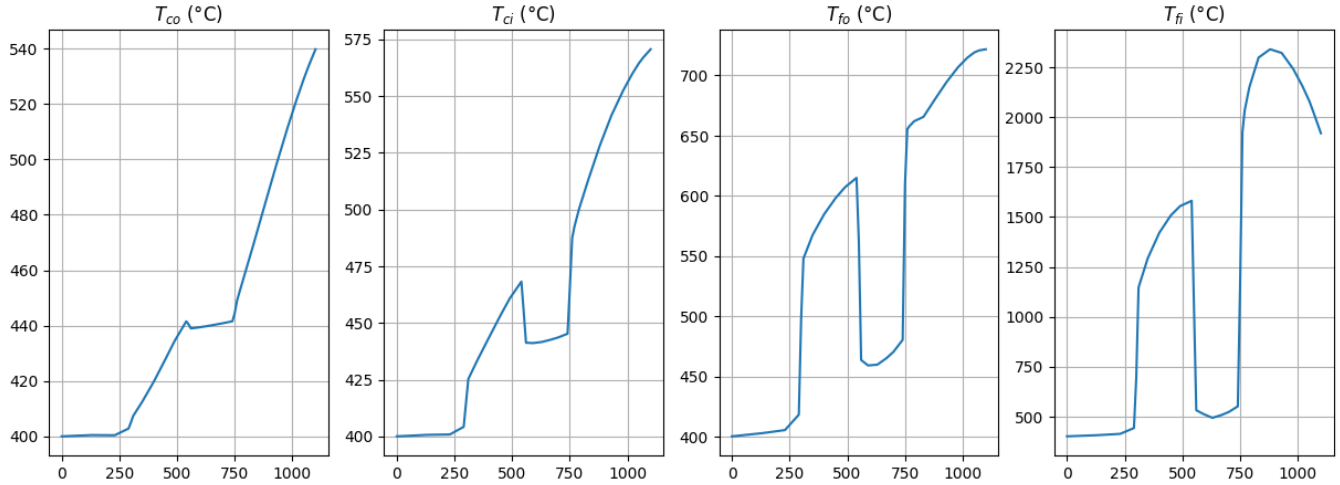

Figure 4: Cladding and fuel temperatures vs pin active length (mm)

As mentioned before, from figure 4 it is evident that the fuel temperature is way lower than the one calculated in cold geometry.
Moreover, in proximity of the higher peak factor (23) a radial profile was made since it is the most critical, allowing to roughly estimate the discrepancy between the two approaches (it is substantial since the temperature is now under the design limit).
Finally, the calculations showed that with a thickness of the cladding greater or equal than 0.58mm there is contact between fuel and cladding just due to thermal expansion. We decided to avoid this condition and so, by keeping

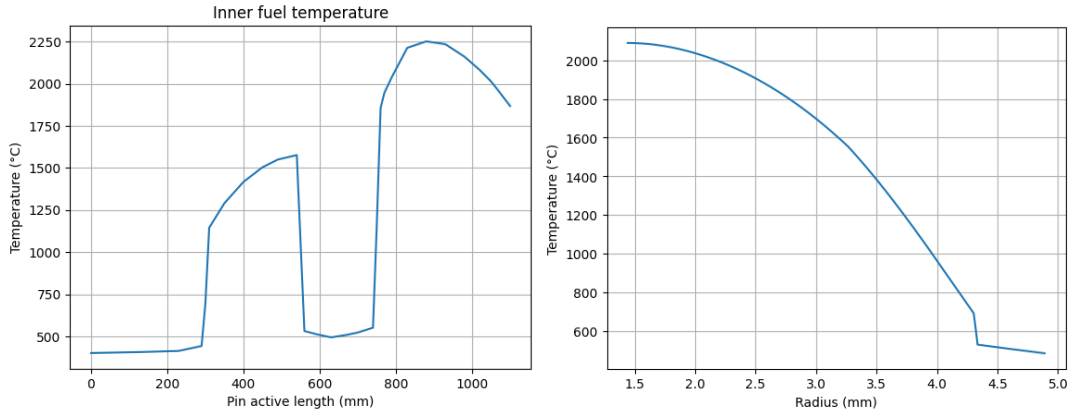

(a) Inner fuel temperature axial profile after fuel restructuring

(b) Hot geometry (after restructuring) radial profile

Figure 5

in mind the lower limit of the cladding's thickness explained before, we can state that the acceptable value of the thickness of the cladding according to our analysis are between 0.53-0.54mm and 0.57mm. All these values have been tested also for all the subsequent calculations, satisfying all the requirements (in this report only 0.55mm was considered).

4 Fuel Restructuring

To account for the complex phenomena that deal with fuel restructuring, we used a simplified model. We identified two regions depending on the temperature of the material: where the temperature is lower than 1600°C we considered the material to be unchanged, while for grater temperatures we assumed that all the porosity of the material would drop to zero and that these voids would migrate to the center of the material. This alteration of the fuel material has two consequences: the variation of thermal resistance and the increment of the inner void radius or eventually its creation. A new temperature profile has been computed. Since the pores migration occurs in a few hours, we assume the burnup to be negligible in the calculation of thermal conductivity of the material. No plutonium redistribution has been considered. In a similar way as before, the new temperature profile leads to a variation in thermal expansion, that would lead to a new temperature profile which would lead to a new restructuring and so on. We iterate this process until a difference of less than 1°C was reached. The final temperature profile is displayed in figure 5a.

5 Fission gas release, pressure and lower plenum design

The choice of the length of the lower and upper plenum is aimed at the ensuring that the inner pin pressure is less than $5MPa$ at the end of the fuel operation, when the pressure is expected to be higher due to the production of gaseous fission products, a fraction around $70 - 90\%$ of which is released from the fuel in the pin for fast reactors. In order to be conservative in the estimation, it was done as if it was 90%. At first, the amount of moles of fission products produced at the end of the burnup were calculated by dividing the energy produced by the energy released per fission. Knowing the branching ratio of the production of gaseous fission products, the final amount of gas was easily calculated. Then, two 2D-arrays of possible volumes, initial (unperturbed) and final (keeping in mind thermal expansion and radiation swelling), each value to a different length of both upper and lower plenum. The initial amount of gas is calculated with the initial volume, pressure and temperature, and it is summed to the fission gas previously calculated. Then, the final volume is used to estimate the final pressure. Since most of the volume is stored in the lower plenum, which is in thermal equilibrium with the coolant at the inlet, we use the inlet temperature to calculate the pressure. Since we approximate the whole gas to be 400°C, the upper plenum is chosen to be as small as possible because the more gas is housed inside of it, the more this approximation loses its validity. Both calculations involving pressure were done using the ideal gas law.
The results are summed up in the figure 6b.

Those results allowed to choose a value of $1250mm$ for the upper plenum, allowing for the axial expansion of the fuel, and $826mm$ for the lower plenum ($2076mm$ in total). In this way, the final maximum pressure is supposed to be around $4.92MPa$ and the total length is consistent with the scheme provided that show a total length of $2130mm$, leaving space for the upper and lower plugs and for a spacer between the plena.

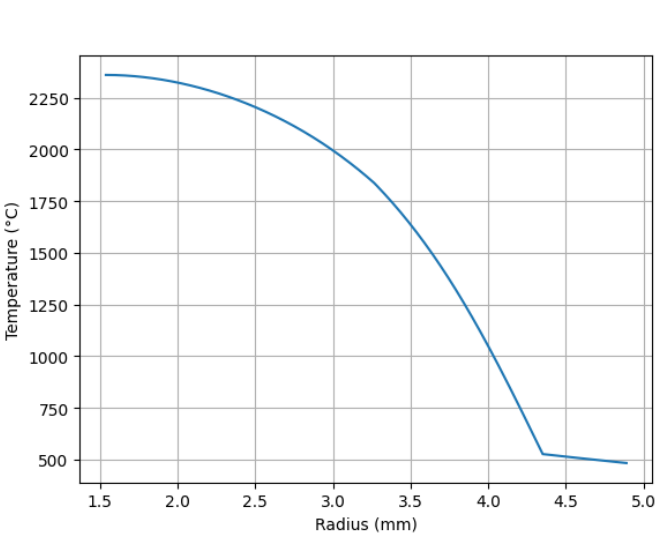

(a) Radial profile for PCI

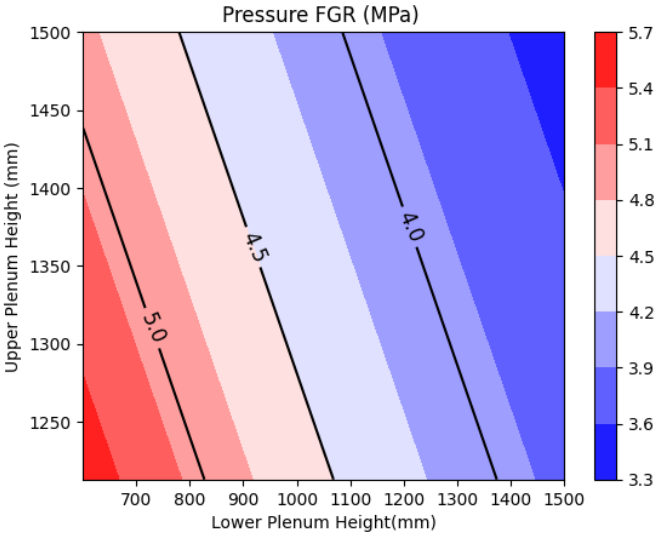

(b) Pressure vs plena lengths

Figure 6

6 Cladding mechanical verification

First of all, it is necessary to verify that the thermal and mechanical stress prior to any pellet-cladding interaction do not strain the steel. All of the following analysis was performed at the twenty-third axial peak factor, deemed to be the most critical since it has the higher linear power. To find the radial stress in both cases the pipe equation was integrated, the hoop stress was found by applying equilibrium equations along the radial direction and the axial stress, in the thermal case, as a sum of radial and hoop stress (in the mechanic cases the axial stress was deemed null). While for the thermal stress estimation the boundary conditions was the radial stress to be null at the inner and outer surfaces, for the mechanical stress it was null at the outer surface (actually there should be the outer pressure but it was both easier and more conservative to neglect it) and $5MPa$ at the inner surface (by choosing the design limit that was imposed as inner pressure we being conservative enough throughout the assembly operation). Since it is considered the linear elastic domain, the mechanical and thermal stresses were summed component wise, and the three components hence found used to find the Von Mises-equivalent stress.

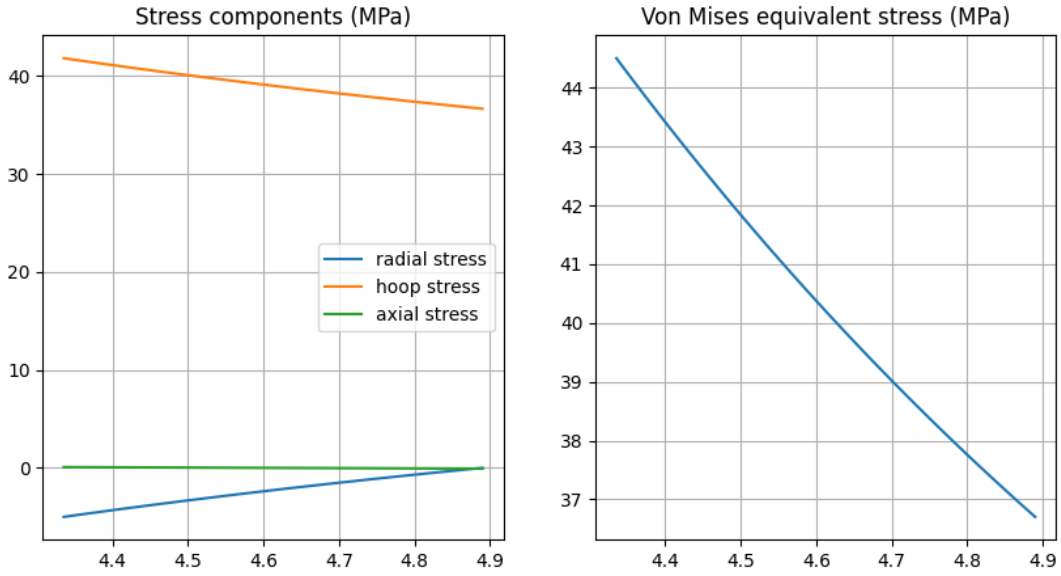

Figure 7: Stresses vs cladding radius (mm)

The results are shown in figure 7.
Since the expected yield stress for the cladding is around $430MPa$, it can be confidently said that the linear elastic

domain is valid.
Moving on to the pellet cladding interaction, in this case it is expected that during the pin operation, the void swelling will lead at a certain point to the contact between cladding and pellet. An array representing the time of operation of the pin day by day was created and the fuel and cladding swelling evaluated every day by a means of a for cycle. On the 161th day of operation, the contact occurs. The pressure was calculated as:

$$P_{contact} = (\frac{i}{b})\frac{1}{\frac{1}{E_{cladding}}(\frac{b^2+c^2}{c^2-b^2} + \frac{1}{\nu_{cladding}}) + \frac{1}{E_{fuel}}(\frac{a^2+b^2}{b^2-a^2} - \frac{1}{\nu_{fuel}})} \tag{3}$$

$$i \simeq \frac{1}{3}(\frac{\Delta V}{V})_{fuel} Rfuel \tag{4}$$

where a, b and c are the inner fuel radius, outer fuel radius (that since contact is equal in that point to the inner cladding radius) and outer cladding radius at the end of the pin operation (when we expect the maximum swelling, hence the maximum stress). This pressure is used exactly like the inner pressure was used previously without PCI. The equivalent stress found is around one hundred times the yielding stress. Clearly, this point in never reached this way. The swelling proceeds and the very next day following the contact the yielding condition of 0.2% strain is reached. Now, the need for a model that describes the evolution of strain arises because we need to verify that the stress, temperature and operation time are low enough to ensure the survival of the cladding up to the end of its operation. The idea is that the stress never reaches these levels because the moment in which the contact happens, or shortly after, the cladding is strained and its deformation, day by day, accommodates the fuel's expansion. Since this calculations turned up to be really complex, some very strong, yet conservative, approximations were made: the power decrease by 10% was not accounted for,neither in temperature nor in neutron flux (for which only its fast component was taken into account) and, after the strain condition has been reached, the equivalent stress is deemed to be constant and equal to the yield stress. For what concerns the temperatures used for the following verification, clearly the contact between cladding and fuel alters the radial temperature profile so a new one was developed. To do so, another approximation was done by imposing that the burnup should be the maximum reached throughout the operation of the pin, lowering the heat conductivity and hence increasing the inner fuel temperature. To calculate the local burnup, it was imposed that it was proportional to the axial peak factor in order to take into consideration the different neutron flux, and that the average should be the target burnup. The resulting radial profile is displayed in figure 6a.
At this point, the first thing to do was to estimate, in this condition, the time needed for the cladding to rupture and to do so, a strain rate needed to be calculated. The phenomena to consider are the void swelling, the thermal creep (since $T_{cladding} \simeq 0.4 \div 0.5 T_{melting}$) and the irradiation creep. So, for what concerns both types of creep the strain rate was calculated by summing the two provided correlations, but the radiation swelling rate was calculated by calculating the final expected value and then dividing it by the number of hours of planned operation.
Under the stated hypotheses, the strain rate is constant and the strain is described by a straight line that begins at the yielding moment with a 0.2% of strain.
The strain that would result in a rupture of the cladding is a function of the temperature of the cladding, and was calculated using the cladding average temperature. It was estimated that this point was reached after around eleven thousand days, which is way more than the required 1440 days of operation. The next step is finding, given the desired time of operation and cladding average temperature, the equivalent stress that would lead to a rupture of the cladding by using the Larson-Miller parameter. This calculation lead to a stress of 460MPa, against the 420MPa of yielding stress that in our (conservative) model describe the equivalent stress withstood by the cladding. The Larson-Miller parameter is used to estimate the temperature that would cause the cladding to rupture given a time of operation and an equivalent stress, which is 524°C against an average design cladding temperature of 505°C.
So, summing up:

- $\frac{T_{rupture}}{T_{design}} = 1.02$
- $\frac{\sigma_{rupture}}{\sigma_{design}} = 1.09$
- $\frac{t_{rupture}}{t_{design}} = 8.37$

Even though the first two ratios are very low, yet greater than one, the conditions under which they were calculated are very conservative.